International Journal of Advance Research in Science and Engineering
Vol. No.6, Issue No. 01 , January 2017
www.ijarse.com
IJARSE
ISSN (O) 2319 - 8354
ISSN (P) 2319 - 8346

CHELATING AGENT ASSISTED SYNTHESIS OF COBALT FERRITE NANOPARTICLES BY SOL-GEL ROUTE

A. Persis Amaliya, S. Anand, S. Pauline

Department of Physics, Loyola College, Chennai – 600034, (India)

ABSTRACT

Nanostructured pure cobalt ferrite (S1) and chelate ethylenediaminetetraacetic acid (EDTA) added cobalt ferrite (S2) crystallites were synthesized with high yield through sol-gel route followed by annealing treatment. Single Phase cubic spinel structure was confirmed by X-ray diffraction (XRD), lattice parameters and crystallite sizes were calculated. Functional groups were confirmed by Fourier transform infrared spectroscopy (FTIR). The micro structural studies done by High resolution scanning electron microscopy (HRSEM) technique showed reduction in agglomeration with the addition of EDTA. Raman active modes are observed from Raman spectra. Hysteresis loops were recorded by Vibrating sample magnetometer (VSM) and no significant changes in saturation magnetization (Ms), coercivity (Hc) and retentivity (Mr) was noted with the addition of EDTA. Electrical properties were studied by Impedance analysis and resistance and capacitance were found to change for EDTA added $CoFe_2O_4$ nanoparticles.

Keywords: ***Cobalt Ferrite, EDTA, Impedance Analysis, Sol-Gel, VSM.***

1. INTRODUCTION

Ferrites have been investigated due to their very basic properties like a significant saturation magnetization; high electrical resistivity, low electrical losses and a very good chemical stability.Ferrites are classified into spinels, hexagonal ferrite and garnets according to their primary crystal lattice [1]. Spinel ferrites have interesting applications like high frequency electronic device components, soil remediation, and medical diagnosis and treatments. Among spinel ferrites**,** research work on cobalt ferrite has been gaining momentum due to its enormous applications in various fields like medicine, data storage devices and magneto-optical devices [2-6]. In medical field, $CoFe_2O_4$ based nanoparticles play an important role as enhancing signal receptor in magnetic resonance imaging (MRI), hyperthermia agents because of their good heat absorption capacity and magnetically tagging devices of bioentities, for bio-separation and drug delivery [7,8].

Different methods have been proposed earlier like (i) Polyol method [9], (ii) Sol gel method [10-12], (iii) Co-precipitation method [13-15], (iv) Hydrothermal method [7], (v) Supercritical hydrothermal method [16], (vi) Microwave method [17] for synthesizing cobalt ferrite nanoparticles. The addition of surfactant in the synthesis of ferrite nanoparticles supports to control the particle growth and agglomeration because of the steric interference and stabilization properties of surfactant. Various surfactants and chelating agents were made to assist the synthesis [17-

IJARSE
ISSN (O) 2319 - 8354
ISSN (P) 2319 - 8346

21]. The present study is on simple preparation of cobalt ferrite nanoparticles by sol-gel method with the assistance of chelant EDTA.

II MATERIALS AND METHOD

2.1. Materials

The raw materials used for sol-gel synthesis of cobalt ferrite nanoparticles were ferric nitrate ($Fe(NO_3)_3.9H_2O$), cobalt nitrate ($Co(NO_3)_2.6H_2O$), ethylene glycol and ethylenediaminetetraacetic acid (EDTA:$C_{10}H_{16}N_2O_8$). All the reagents used for the synthesis of cobalt ferrite nanoparticles were analytical grade and used as received from Merck without further purification.

2.2. Synthesis Procedure

Sample (S1) was synthesized via sol-gel route using cobalt nitrate, ferric nitrate and ethylene glycol. Metal nitrates were used as metal precursors and oxidizing agents and ethylene glycol as a reducing agent and fuel for the synthesis. Typically cobalt nitrate and ferric nitrate were taken in the mole ratio 1:2. Required quantity of ethylene glycol [$(C_2H_4 (OH)_2$] was added and stirred to get clear solution. This solution was transferred to a hot plate and heated around 60º-80ºC. The obtained gel was transferred to a silica crucible and heated for 2 hours at 200ºC. The resultant powder was calcined for 3 hours at 600ºC and fine black powder was obtained. Sample S2 was synthesized by the same procedure given above with added EDTA. The word "chelate" comes from the Greek word "Chelae" which means claw. Chelating agent EDTA has large molecules that will bind to another molecule usually of metal, surrounding it and removing it from further reactivity.

III RESULTS AND DISCUSSION

3.1. X-Ray Diffraction (XRD) Analysis

The formation of cobalt ferrite nanoparticles was analyzed by XRD technique using a SIEMENS D-5000 X-Ray diffractometer (Cu-Kα radiation with λ = 1.54056 Å). Figure 1 shows the plot between Bragg's angle 2θ and the intensity of X-ray used. All the peaks in the pattern well match with JCPDS file 22-1086. The formation of cubic spinel structure was evident from the XRD pattern.

Lattice parameters for the spinel phase were calculated using the formula

$$a = d\sqrt{(h^2+k^2+l^2)}\ (Å)$$

Where, 'd' is inter planar distance and h, k, l are the Miller indices of the crystal planes.

Crystallite size was calculated using Scherer relation

$$D = \frac{0.9\lambda}{\beta \cos\theta}\ (nm)$$

Where, D is the crystallite size, β is the full width at half maximum (FWHM), λ is the X-ray wavelength and θ is the Bragg's angle.

International Journal of Advance Research in Science and Engineering
Vol. No.6, Issue No. 01 , January 2017
www.ijarse.com
IJARSE
ISSN (O) 2319 - 8354
ISSN (P) 2319 - 8346

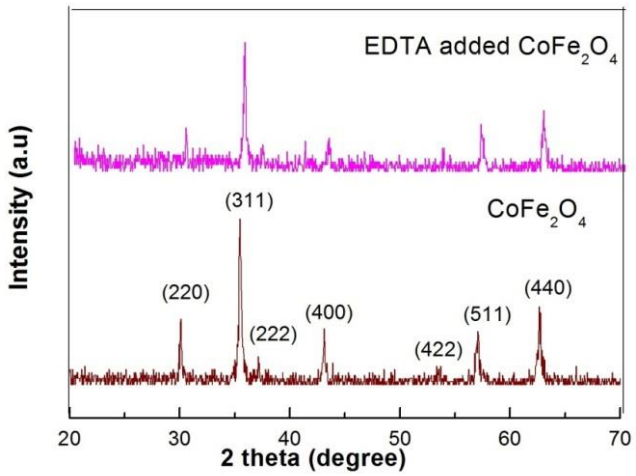

Figure 1. XRD pattern of pure $CoFe_2O_4$ and EDTA assisted $CoFe_2O_4$ nanoparticles.

Cell volume was calculated by following relation

$$V = a^3 (cm^3)$$

Where,'*a*' is the lattice constant.

X-ray density was calculated by given formula

$$d_x = \frac{8M}{Na^3} (g/cm^3)$$

Where M is the molecular weight, N is the Avogadro's number and 'a' is the lattice constant. All the calculated values from XRD data are tabulated below.

Table 1. Crystallite grain size (D), Lattice parameter (a), Cell volume (V) and X-ray density (d_x) of the prepared samples.

Entry	Sample	Average Crystallite size (D) nm	Lattice parameter(a) Å	Cell volume (V) cm^3	X-ray density $(d_x)\times10^{-23} g/cm^3$
1	$CoFe_2O_4$(S1)	34	8.3841	589.3446	4.4334
2	$CoFe_2O_4$+EDTA(S2)	34	8.3887	590.3152	4.4285

Since lattice parameter is the measure of length between two edges of lattice, cell volume is slightly increasing for EDTA added cobalt ferrite which has higher lattice parameter compared to pure cobalt ferrite. X-ray density decreases with the addition of EDTA. Grain size of samples S1 and S2 is almost same and so lattice parameter is

IJARSE
ISSN (O) 2319 - 8354
ISSN (P) 2319 - 8346

also almost same for them. Crystallite size found to increase when calcined at high temperature by few authors [20, 22]. According to our findings Crystallite size does not change due to low calcined temperature and less amount of EDTA added.

3.2. Fourier Transform Infrared Spectroscopy Analysis

The FT-IR spectra shown in figure 2 have all the characteristic bands of $CoFe_2O_4$. Absorption bands attributed to the spinel structure ($v1$&$v2$) are found to be around 580 cm^{-1} and 410 cm^{-1} respectively. The modes $v1$and $v2$ are attributed to the cationic vibrations in both octahedral (B) and tetrahedral (A) site of the spinel structure respectively. A band around 1120 cm^{-1} corresponds to Fe-Co alloy; band around 3400 cm^{-1} and 1590 cm^{-1} belongs to O-H stretching vibration, O-H distorted vibration respectively because of adsorbed water by the surface of $CoFe_2O_4$ nanoparticles. Bands at 2916 cm^{-1} and 2352 cm^{-1} are assigned to asymmetric and symmetric stretching of CH_2 groups. The above results well go with the results reported by S. Arokiyaraj et al [23].

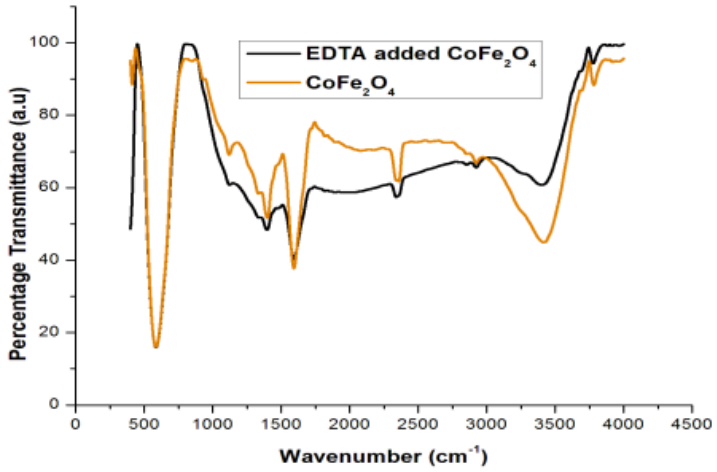

Figure 2. FTIR pattern of pure $CoFe_2O_4$ and EDTA assisted $CoFe_2O_4$ nanoparticles

3.3. High Resolution Scanning Electron Microscopy (HRSEM) Analysis

The morphology of the as synthesized cobalt ferrite nanoparticles was investigated through High Resolution Scanning Electron Microscope (HRSEM, Quanta 200 FEG). From the figure 3, it can be known that the obtained nanoparticles are spherical in shape. When surfactant or chelate is not used, the particles are slightly agglomerated and when EDTA is used agglomeration is reduced.

International Journal of Advance Research in Science and Engineering
Vol. No.6, Issue No. 01 , January 2017
www.ijarse.com
IJARSE
ISSN (O) 2319 - 8354
ISSN (P) 2319 - 8346

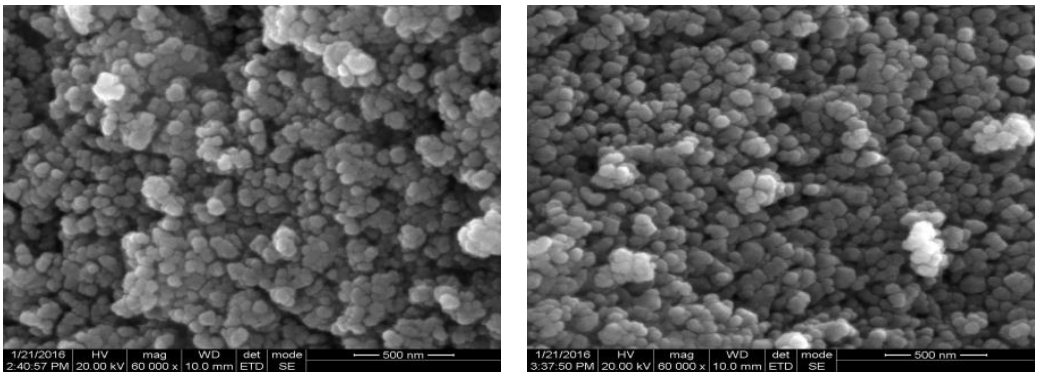

Figure 3. HRSEM images of pure $CoFe_2O_4$ (a) and EDTA assisted $CoFe_2O_4$ (b) nanoparticles

3.4. Raman Spectroscopy Analysis

Raman spectroscopy is a widely used technique which needs powerful laser. The laser photon scattered by molecules of the sample loses or gains energy and it correspond to particular bond in the molecule. Raman spectrum is said to be finger print of a particular substance. Raman spectra of the as prepared samples are given in figure. 4.

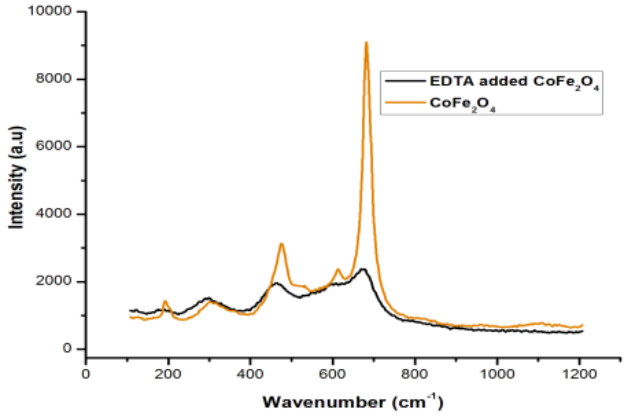

Figure 4. Raman spectra of pure $CoFe_2O_4$ and EDTA assisted $CoFe_2O_4$ nanoparticles

Five Raman active modes of cobalt ferrite $3T_{2g}$, E_g and A_{1g} are observed in the spectrum of samples S1 and S2. E_g and $T_{2g}(3)$ modes correspond to the symmetric and anti-symmetric bending of oxygen atom in (Fe-O and Co-O) bond at octahedral site. A_{1g} mode is attributed to the motion of oxygen atom around metal ions (Co^{2+}-O, Fe^{3+}-O) in the tetrahedral sites. $A_{1g}(2)$ sub-band (~620cm^{-1}) is splitted from $A_{1g}(1)$ band (~680cm^{-1}) and it is caused by partial redistribution of cations [24]. There are slight changes in the wave numbers corresponding to Raman modes of EDTA added sample compared with pure sample. Intensity of peaks reduces with the addition of EDTA. Increase in

IJARSE
ISSN (O) 2319 - 8354
ISSN (P) 2319 - 8346

Table 2. Observed Raman modes for the samples S1, S2

Entry	Assigned Raman modes	S1 wavenumber(cm^{-1})	S2 Wavenumber(cm^{-1})
1	$T_{1g}(3)$	192	190
2	E_g	302	299
3	$T_{1g}(2)$	475	462
4	$T_{1g}(1)$	569	562
5	$A_{1g}(2)$	612	620
6	$A_{1g}(1)$	682	675

intensity with the increase in CTAB concentration is reported by Vadivel et al [25]. Less amount of EDTA may be the cause of decrease in peak intensity.

3.5. Vibrating Sample Magnetometer (VSM) Analysis

Magnetic behavior of $CoFe_2O_4$ nanoparticles was investigated by vibrating sample magnetometer **(**Lakeshore VSM 7410**)**. Hysteresis loops measured at room temperature in figure 5 indicates the ferromagnetic behavior of as prepared samples. Measured values from hysteresis loop are listed in a table.

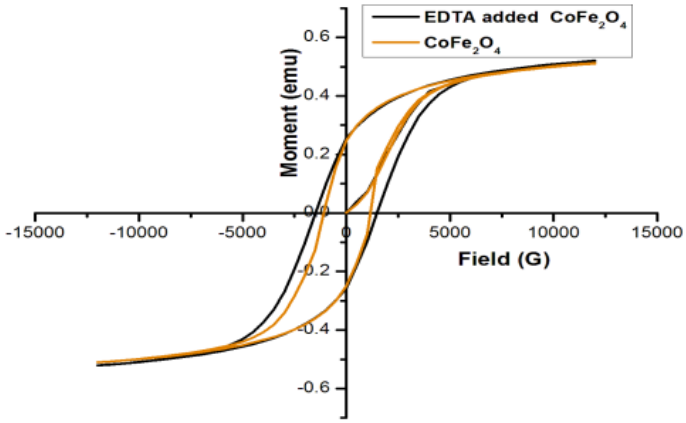

Figure 5. Hysteresis loops of pure $CoFe_2O_4$ and EDTA assisted $CoFe_2O_4$

Saturation magnetization (M_s) is the magnitude of magnetization at which all the moments are aligned. Remanent magnetization (M_r) is the magnitude of magnetization present after saturation and the subsequent removal of the field. Coercivity (H_{ci}) is the magnitude of field required to bring the net magnetization back to zero after field is applied in the direction opposite to the remanent magnetization to randomize magnetic moments [26].

IJARSE
ISSN (O) 2319 - 8354
ISSN (P) 2319 - 8346

Table 3. Coercivity, Saturation magnetization and Remanent magnetization of as prepared samples.

Sample	Coercivity (H_{ci}) Guass	Magnetization (M_s) emu/g	Remanent magnetization(M_r) emu/g
S1	1113	51.176	24.834
S2	1489	52.104	25.615

There was no noteworthy change in magnetic properties. Enhancement in magnetic properties was reported earlier by few researchers [20, 22].

3.6. Impedance Analysis

This study is to know the impedance which can be given by the as synthesized samples. Complex impedance plots of impedance data for the samples S1 and S2 are given below. It is a frequency dependent plot versus impedance (real) along X-axis and impedance (imaginary) along Y-axis. For pure cobalt ferrite two resolved semicircles are seen. The arc at low frequency is of grain boundary and arc at high frequency is of grain. But for EDTA added cobalt ferrite the semicircles are not resolved and considered as single arc. This implies that the contribution of grain boundary dominates the contribution of grain or we may say both cannot be separated.

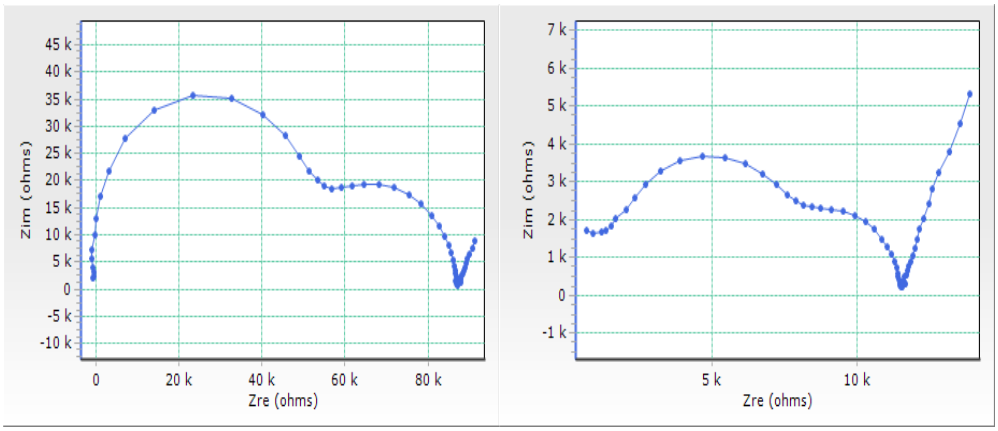

Figure 6. Complex impedance plot of pure $CoFe_2O_4$ and EDTA assisted $CoFe_2O_4$

Resistance from grain (R_g), resistance from grain boundary (R_{gb}), frequency at the peaks of the semicircles for grain (ω_g) and grain boundary (ω_{gb}) were noted directly from the plot. Resistances observed from the plot are nothing but the intercepts of semicircle on X-axis. Capacitance from grain boundary (C_{gb}) and from grain (C_g) was calculated using the following relations [27]

$$C_{gb} = \frac{1}{R_{gb}\omega_{gb}}$$

International Journal of Advance Research in Science and Engineering
Vol. No.6, Issue No. 01 , January 2017
www.ijarse.com
IJARSE
ISSN (O) 2319 - 8354
ISSN (P) 2319 - 8346

$$C_g = \frac{1}{R_g \omega_g}$$

Relaxation time for grain boundary (τ_{gb}) and grain(τ_g) were calculated using the below equations

$$\tau_{gb} = \frac{1}{\omega_{gb}} = C_{gb} R_{gb}.$$

$$\tau_g = \frac{1}{\omega_g} = C_g R_g$$

The complex impedance $Z(\omega)$ of a system at an applied frequency (ω) can be written as the sum of real and imaginary part as given below

$$z(\omega) = z' + jz''$$

Where Z' and Z'' can be written as,

$$z' = \frac{R_g}{1+\omega_g^2 C_g^2 R_g^2} + \frac{R_{gb}}{1+\omega_{gb}^2 C_{gb}^2 R_{gb}^2} \text{ and}$$

$$z'' = \frac{-R_g^2 \omega_g C_b}{1+\omega_g^2 C_g^2 R_g^2} + \frac{-R_{gb}^2 \omega_{gb} C_{gb}}{1+\omega_{gb}^2 C_{gb}^2 R_{gb}^2}$$

The parameters calculated from Complex impedance plot are listed in table 4.

Table 4: Calculated R, C, τ values for grain and grain boundary

Sample	R_{gb} (Ω)	C_{gb} (F)	τ_{gb} (s)	R_g (Ω)	C_g (F)	τ_g (s)
S1	59078	2.6827E-10	1.5849E-5	87060	2.2918E-9	1.9952E-4
S2	87356	2.2840E-10	1.9952E-5	-	-	-

Grain boundary resistance of sample S2 is high when compared to that of sample S1. Thus when EDTA is added grain boundary resistance increases and capacitance decreases.

4. CONCLUSION

Pure $CoFe_2O_4$ nanoparticles and $CoFe_2O_4$ nanoparticles with chelate EDTA were successfully prepared by sol-gel method with high yield. XRD analysis confirmed the cubic spinel structure of the samples. Both crystallite size and lattice parameter remained more or less same when EDTA is present when compared that of pure $CoFe_2O_4$. FTIR pattern revealed the functional groups in CoFe2O4. Nearly spherical ferromagnetic nanoparticles were obtained. Raman spectra well matched with previous studies. Thus the present work concludes that chelant reduces agglomeration and have no effect on reducing particle size and magnetic property. Grain boundary found to increase with the addition of EDTA.

IJARSE
ISSN (O) 2319 - 8354
ISSN (P) 2319 - 8346

Acknowledgement:

The Authors are thankful to Dept. of Nuclear Physics, University of Madras, Chennai and SAIF, IITM, Chennai for XRD and HRSEM facilities.

REFERENCES

1) Berenice Cruz-Franco, Thomas Gaudisson, SouadAmmar, Ana Maria Bolarin-Miro, Felix Sanchez de Jesus, Frederic Mazaleyrat, Sophie Nowak, Gabriela Vazquez-Victorio, Raul Ortega-Zempoalteca, and Raul Valenzuela, Magnetic Properties of Nanostructured Spinel Ferrites, IEEE Transactions on Magnetics, 50(4) April 2014.
2) Schmid G, Nanoparticles: from theory to application, Weinheim: Wiley-VCH, second edition, 2004.
3) Jordan A, Scholz R, Wust P, Endocytosis of dextran and silan-coated magnetite nanoparticles and the effect of intracellular hyperthermia on human mammary carcinoma cells in vitro, J.Magn.Magn.Mater, 194 (1999) 185-96.
4) Kim DH, Nikles DE, Johnson DT, Brazel CS, Heat generation of aqueously dispersed $CoFe_2O_4$ nanoparticles as heating agents for magnetically activated drug delivery and hyperthermia, J.Magn.Magn. Mater, 320 (2008) 2390-2396.
5) Mornet S, Vasseur S, Grasset F, Duguet E, Magnetic nanoparticle design for medical diagnosis and therapy, J. Mater Chem., 14 (2004) 2161-2175.
6) Wada S, Tazawa K, Furuta I, Nagae H. Antitumor, Effect of new local hyperthermia using dextran magnetite complex in hamster tongue carcinoma, Oral Dis, 9(4), (2003) 218-223.
7) Violetta Georgiadou, Chrysoula Kokotidou, Benjamin Le Droumaguet, Benjamin Carbonnier, Theodora Choli-Papadopoulou and Catherine Dendrinou-Samara, Unveiling the Physicochemical Features of $CoFe_2O_4$ NPs Synthesized via a Variant Hydrothermal Method: NMR Relaxometric Properties, The Royal Society of Chemistry, Dalton Trans., 43(2014) 6377- 6388.
8) Valerie Cabuil, Vincent Dupuis, Delphine Talbot, Sophie Neveu, Ionic magnetic fluid based on cobalt ferrite nanoparticles: Influence of hydrothermal treatment on the nanoparticle size, Journal of Magnetism and Magnetic Materials, 323 (2011) 1238–1241.
9) Amal M. Ibrahim, M.M. Abd El-Latif , Morsi M. Mahmoud, Synthesis and characterization of nano-sized cobalt ferrite prepared via polyol method using conventional and microwave heating techniques, Journal of Alloys and Compounds, 506 (2010) 201–204.
10) Mojtaba Nasr-Esfahani and AzaliaAzlegini, The Effect of Citric Acid and Ethylene Glycol Mole Ratios on the Microstructure and Magnetic Properties of Z-Type Hexagonal Ferrite Nano Powder Prepared by Sol-Gel Method, IPCBEE vol.25(2011), IACSIT Press, Singapore.

IJARSE
ISSN (O) 2319 - 8354
ISSN (P) 2319 - 8346

11) Noppakun Sanpo, James Wang and Christopher C. Berndt, Influence of Chelating Agents on the Microstructure and Antibacterial Property of Cobalt Ferrite Nanopowders, Journal of the Australian Ceramic Society, Volume 49 (1) (2013) 84 – 91.

12) S. Kanagesan, M. Hashim, S. Tamilselvan, N.B. Alitheen, I. Ismail, M.Syazwan, M.M.M. Zuikimi, Sol-gel auto-combustion synthesis of cobalt ferrite and it's cytotoxicity properties, Digest Journal of Nanomaterials and Biostructures, 8(4) (2013) 1601 – 1610.

13) Yue Zhang, Zhi Yang, Di Yin, Yong Liu, Chun Long Fei, Rui Xiong, Jing Shi, Gao Lin Yan, Composition and magnetic properties of cobalt ferrite nanoparticles prepared by the co-precipitation method, Journal of Magnetism and Magnetic Materials, 322 (2010) 3470–3475.

14) M.A.G. Soler, T.F.O. Melo, S.W. da Silva, E.C.D. Lima, A.C.M. Pimenta, V.K. Garg, A.C. Oliveira, P.C. Morais, Structural stability study of cobalt ferrite-based nanoparticles using micro Raman spectroscopy, Journal of Magnetism and Magnetic Materials, 272–276 (2004) 2357–2358.

15) G.A. El-Shobaky, A.M. Turky, N.Y. Mostafa, S.K. Mohamed, Effect of preparation conditions on physicochemical, surface and catalytic properties of cobalt ferrite prepared by co-precipitation, Journal of Alloys and Compounds, 493 (2010) 415–422.

16) D. Zhao, X. Wu, H. Guan, E. Han, Study on supercritical hydrothermal synthesis of $CoFe_2O_4$ nanoparticles, J. of Supercritical Fluids 42 (2007) 226–233.

17) F. Bensebaa, F. Zavaliche, P.L. Ecuyer, R.W Cochrane, T Veres, Microwave synthesis and characterization of Co–ferrite nanoparticles, Journal of Colloid and Interface Science, 227(1), (2004) 104-110.

18) G.B. Ji, S.L. Tang, S.K. Ren, F.M. Zhang, B.X. Gu, Y.W. Du, Simplified synthesis of single-crystalline magnetic $CoFe_2O_4$ nanorods by a surfactant-assisted hydrothermal process, Journal of Crystal Growth, 270 (2004) 156–161.

19) Katalin Sinko, Eniko Manek, Aniko Meiszterics, Karoly Havancsak, Ulla Vainio, Herwig Peterlik, Liquid-phase syntheses of cobalt ferrite nanoparticles, J. Nanopart. Res., 14 (2012) 894.

20) L. Avazpour, M.A. Zandikhajeh, M.R. Toroghinejad, H. Shokrollahi, Synthesis of single-phase cobalt ferrite nanoparticles via a novel EDTA/EG precursor-based route and their magnetic properties Journal of Alloys and Compounds,637 (2015) 497–503.

21) H. Hajihashemi, P. Kameli, H. Salamati, The Effect of EDTA on the Synthesis of Ni Ferrite Nanoparticles, J.Supercond. Nov.Magn. 25 (2012) 2357–2363.

22) Pham D. Thang, Guus Rijnders, Dave H.A. Blank, Spinel cobalt ferrite by complexometric synthesis, Journal of Magnetism and Magnetic Materials 295 (2005) 251–256.

23) S. Arokiyaraj, M. Saravanan, N.K. Udaya Prakash, M. Valan Arasu, B. Vijayakumar, S. Vincent, Enhanced antibacterial activity of iron oxide magnetic nanoparticles treated with Argemonemexicana L. leaf extract: an in vitro study, Materials Research Bulletin 48 (2013) 3323–3327.

IJARSE
ISSN (O) 2319 - 8354
ISSN (P) 2319 - 8346

24) P. Chandramohan, M.P. Srinivasan, S. Velmurugan, S.V. Narasimhan, Cation distribution and particle size effect on Raman spectrum of $CoFe_2O_4$, Journal of Solid State Chemistry, 184 (2011) 89–96.

25) M. Vadivel, R. RameshBabu, K. Ramamurthi and M. Arivanandhan, CTAB cationic surfactant assisted synthesis of $CoFe_2O_4$ magnetic nanoparticles, Ceramics International, 42(2016) 19320-19328.

26) Natalie A. Frey, Sheng Peng, Kai Cheng and Shouheng Sun, Magnetic nanoparticles: synthesis, functionalization, and applications in bioimaging and magnetic energy storage, Chem. Soc. Rev., 38 (2009) 2532–2542.

27) A.M.M. Farea, Shalendra Kumar, Khalid Mujasam Batoo, Ali Yousef, Chan Gyu Lee, Alimuddin, Structure and electrical properties of $Co_{0.5}CdxFe_{2.5-x}O_4$ ferrites, Journal of Alloys and Compounds 464 (2008) 361–369.